Inorganica Chimica Acta 400 (2013) 20–25

Contents lists available at SciVerse ScienceDirect

Inorganica Chimica Acta

journal homepage: www.elsevier.com/locate/ica

Synthesis and structural characterization of asymmetric mononuclear ruthenium (II) complexes derived from 2-(1,2,3-thiadiazol-4-yl)pyridine and azoimine ligands

Mousa Al-Noaimi [a,*], Mohammad El-khateeb [b,1], Ismail Warad [c], Salim F. Haddad [d]

[a] Department of Chemistry, Hashemite University, P.O. Box 150459, Zarqa – 13115, Jordan
[b] Department of Chemistry, College of Sciences and Arts at Alkamil Campus, King Abdulaziz University, Saudi Arabia
[c] Department of Chemistry, AN-Najah National University, Nablus, Palestinian Territories, Palestine
[d] Chemistry Department, Faculty of Science, University of Jordan, Amman, Jordan

ARTICLE INFO

Article history:
Received 20 July 2012
Received in revised form 2 February 2013
Accepted 4 February 2013
Available online 15 February 2013

Keywords:
Ruthenium
Azoimine
Electrochemistry
DFT calculation

ABSTRACT

Five mononuclear ruthenium complexes of the general type *trans*-[Ru^{II}(L)(Azo)Cl_2] {(Azo = $C_6H_5N{=}NC(COCH_3){=}NC_6H_4Y$, Y = H (**1**), CH_3 (**2**), OCH_3 (**3**), Cl (**4**), Br (**5**)} and L is 2-(1,2,3-thiadiazol-4-yl)pyridine have been synthesized and their structures investigated by elemental analyses, spectroscopic (IR, UV–Vis, and NMR) and electrochemical (cyclic voltammetry) techniques. In addition, complex (**3**) has been further characterized by X-ray diffraction analysis. The absorption spectrum of **3** in acetonitrile has been modeled by time-dependent density functional theory (TD-DFT) using mixed basis set, LanL2DZ/6-31+g(d,p), in acetonitrile as a solvent.

1. Introduction

Since the discovery of 2,2′-bipyridine (bpy) last century [1], the chemistry of this ligand has been extensively used in coordination and organometallic chemistry and has been shown to coordinate to almost all metals in the periodic table [2]. For many years, we have been involved in the syntheses and studies of mixed-ligand ruthenium complexes of azoimine and chelating heterocyclic ligands related to 2,2′-bipyridine (bpy) [3–8]. Replacing one or both of the pyridine rings in bpy with other nitrogen-containing heterocycles leads to significant changes in the physicochemical properties of the resultant metal complexes [9–12]. Heterocycles that have commonly been employed for this purpose include π-deficient azines, such as pyrazines and pyridazines, and benzo-fused analogues, such as quinolines and quinoxalines [9]. π-Excessive azoles have also been extensively used, with pyrazoles, imidazoles, thiazoles and their benzo analogues which proved particularly popular [9]. Among the various classes of biologically active coordination compounds and their complexes, thiadiazoles have attracted considerable attention [10–12]. Thiadiazoles are largely used as antibacterial [13], antifungal [14], and antitumor agents [15,16]. As ligands, they also provide many potential binding sites [17–20] for complexation and have obtained a diverse biological activity by the result of such chelation.

Herein, the novel family of the mononuclear mixed-ligand ruthenium complexes of the type *trans*-[Ru^{II}(L)(Azo)Cl_2] {(Azo = $C_6H_5N{=}NC(COCH_3){=}NC_6H_4Y$, Y = H (**1**), CH_3 (**2**), OCH_3 (**3**), Cl (**4**), Br (**5**)) and L is 2-(1,2,3-thiadiazol-4-yl)pyridine has been prepared to study the effect of replacing one of the pyridine ring of the 2.2′-bipyrdine with a more π-excessive 1,2,3-thiadiazole ring and the substituent Y of the azoimine ligand on the electronic properties of the resulting mononuclear ruthenium complexes. Also, we describe herein spectral, electrochemical and structural characterization of a representative ruthenium complex.

2. Materials

The reagents: ruthenium trichloride, lithium chloride, tetrabutylammonium hexafluorophosphate (TBAHF), and solvents (reagent grade) were purchased from Aldrich. Ethyl carbazate [21] and azoimine ligands (Azo) [3] were prepared following reported procedure. 2-(1,2,3-Thiadiazol-4-yl)pyridine) (L) was prepared as described previously [22] with some modification.

* Corresponding author. Tel.: +962 5 3903333; fax: +962 5 3826613.
E-mail address: manoaimi@hu.edu.jo (M. Al-Noaimi).
[1] Permanent address: Department of Chemistry, Jordan University of Science and Technology, Irbid 22110, Jordan.

0020-1693/$ - see front matter © 2013 Elsevier B.V. All rights reserved.
http://dx.doi.org/10.1016/j.ica.2013.02.003

2.1. Syntheses

2.1.1. Synthesis of 2-(1,2,3-thiadiazol-4-yl)pyridine (L)

A mixture of 2-acetylpyridine (3.02 g, 25 mmol), ethyl carbazate (2.60 g, 25 mmol), 2.0 mL acetic acid and ethanol (100 mL) was boiled under reflux for 24 h. The solvent was removed and the white formed precipitate was collected and washed with diethyl ether. The precipitate was placed in a light-protected 150 cm^3 two-neck round bottom flask and cooled on a water-ice bath. $SOCl_2$ (30 mL) was added dropwise. The water-ice bath was removed, and the solution was allowed to warm to 40 °C for 48 h. During the reaction time, the solution turned dark brown which slowly became white and a solid material was formed in the solution. The excess $SOCl_2$ was removed by simple distillation and 50 mL of toluene was added to the residue. The product was collected and washed with diethyl ether to give a brown solid product, Yield (2.91 g, 85%).

2.1.2. General procedure for the syntheses of trans-[Ru^{II}(L)(Azo)Cl_2]

Ruthenium trichloride trihydrate (0.26 g, 1.0 mmol) and (1.0 mmol) of (Azo) ligand were dissolved in 100 mL of absolute ethanol in a 250 mL two-necked light-protected flask fitted with a dinitrogen inlet tube. The solution was flushed with dinitrogen and refluxed for 1 h. Afterwards 1.0 mmol of 2-(1,2,3-thiadiazol-4-yl)pyridine (**L**) was added to the solution. The reaction was heated for an additional 3 h then the solvent was removed by a rotary evaporator. The crude product was dissolved in dichloromethane and purified by alumina grade (III). Acetone was used to elute the second dark-red band of the product.

2.1.2.1. trans-[Ru(C_6H_5N=NC($COCH_3$)=NC_6H_5)(L)Cl_2] (1). Yield (0.275 g, 47%). UV–Vis. in acetonitrile: λ_{max}(nm) (ε_{max}, M^{-1} cm^{-1}): 505 (7.57×10^3), 384 (8.96×10^3), 327 (11.47×10^3). I.r. (KBr, cm^{-1}): $\nu_{N=N}$ = 1480, $\nu_{C=N}$ = 1601, $\nu_{C=O}$ = 1692. ^{1}H NMR (DMSO) δ: 10.14 (1H, d, H14), 8.14 (1H, t, H12), 7.99 (1H, d, H11), 7.94 (1H, s, H10), 7.91 (1H, d, H5), 7.83 (1H, t, H13), 7.65 (1H, t, H8), 7.64 (1H, t, H7),7.52 (2H, m, H6, H9), 7.37 (2H, m, H1, H4), 7.26 (2H, m, H3, H2), 2.37 (3H, s, $COCH_3$). Calc. for $RuC_{22}H_{18}N_6OCl_2S$: C, 45.06; H, 3.09; N, 14.33. Found: C, 45.21; H, 3.23; N, 14.42%.

2.1.2.2. trans-[Ru(C_6H_5N=NC($COCH_3$)=$NC_6H_4CH_3$)(L)Cl_2] (2). Yield (0.246 g, 41%). UV–Vis. in acetonitrile: λ_{max}(nm) (ε_{max}, M^{-1} cm^{-1}): 503 (7.90×10^3), 375 (8.88×10^3), 330 (11.04×10^3). I.r. (KBr, cm^{-1}): $\nu_{N=N}$ = 1476, $\nu_{C=N}$ = 1601, $\nu_{C=O}$ = 1692. ^{1}H NMR ($CDCl_3$) δ: 10.14 (1H, d, H14), 8.53 (1H, t, H12), 8.15 (1H, d, H11), 8.98 (1H, d, H5), 7.89 (1H,d, H9), 7.64 (2H, m, H13, H8), 7.65 (1H, d, H3), 7.51 (1H, d, H2), 7.32 (2H, m, H6, H7), 7.26 (1H, s, H10), 7.18 (2H, m, H1, H4), 2.63 (3H, s, $COCH_3$), 2.63 (3H, s, CH_3). Calc. for $RuC_{23}H_{20}N_6OCl_2S$: C, 46.00; H, 3.36; N, 14.00.Found: C, 46.21; H, 3.23; N, 14.12%.

2.1.2.3. trans-[Ru(C_6H_5N=NC($COCH_3$)=$NC_6H_4OCH_3$)(L)Cl_2] (3). Yield (0.271 g, 44%). UV–Vis in acetonitrile: λ_{max}(nm) (ε_{max}, M^{-1} cm^{-1}): 507 (6.50×10^3), 383 (8.68×10^3), 326 (10.75×10^3). I.r. (KBr, cm^{-1}): $\nu_{N=N}$ = 1470, $\nu_{C=N}$ = 1590, $\nu_{C=O}$ = 1697. ^{1}H NMR (DMSO) δ:10.13 (1H, d, H14), 8. 52 (1H, t, H12), 8.13 (1H, d, H11), 7.96 (1H, d, H5), 7.87 (1H, d, H9), 7.80 (1H, t, H13), 7.71(1H, t, H8), 7.63 (1H, d, H3), 7.61 (1H, d, H2), 7.49 (1H, t, H6), (1H, s, H10), 7.29 (1H, t, H7), 7.07 (1H, d, H1), 6.94 (1H, d, H4), 3.81 (3H, s, OCH_3), 2.70 (3H, s, $COCH_3$). *Anal.* Calc. for $RuC_{23}H_{20}N_6O_2Cl_2S$: C, 44.81; H, 3.27; N, 13.63. Found: C, 44.77; H, 3.18; N, 13.52%.

2.1.2.4. trans-[Ru(C_6H_5N=NC($COCH_3$)=NC_6H_4Cl)((L)Cl_2] (4). Yield (0.236 g, 38%). UV–Vis in acetonitrile: λ_{max}(nm) (ε_{max}, M^{-1} cm^{-1}): 509 (7.97×10^3), 395 (9.31×10^3), 323 (10.33×10^3). I.r. (KBr, cm^{-1}): $\nu_{N=N}$ = 1489, $\nu_{C=N}$ = 1587, $\nu_{C=O}$ = 1694. ^{1}H NMR (DMSO) δ:10.17 (1H, d, H14), 8. 56 (1H, t, H12), 8.17 (1H, d, H11), 8.00 (1H, d, H5), 7.91 (1H, d, H9), 7.84 (1H, t, H13), 7.75(1H, t, H8), 7.65 (1H, d, H3), 7.61 (1H, d, H2), 7.52 (1H, t, H6), 7.46 (1H, t, H7), 7.37 (1H, s, H10), 7.30 (1H, d, H1), 7.26 (1H, d, H4), 2.70 (3H, s, $COCH_3$). *Anal.* Calc. for $RuC_{22}H_{17}N_6O_2Cl_3S$: C, 42.56; H, 2.76; N, 13.54. Found: C, 42.47; H, 2.88; N, 13.42%.

2.1.2.5. trans-[Ru(C_6H_5N=NC($COCH_3$)=NC_6H_4Br)(L)Cl_2] (5). Yield (0.232 g, 35%). UV–Vis in acetonitrile: λ_{max}(nm) (ε_{max}, M^{-1} cm^{-1}): 511 (8.09×10^4), 392. (8.29×10^3), 316 (11.95×10^3). I.r. (KBr, cm^{-1}): $\nu_{N=N}$ = 1479, $\nu_{C=N}$ = 1593, $\nu_{C=O}$ = 1705. ^{1}H NMR (DMSO) δ:10.16 (1H, d, H14), 8. 54 (1H, t, H12), 8.17 (1H, d, H11), 7.99 (1H, d, H5), 7.91 (1H, d, H9), 7.84 (1H, t, H13), 7.74 (1H, d, H2), 7.65 (1H, d, H3), 7.62 (1H, s, H10), 7.59 (1H, d, H1), 7.52 (1H, t, H6), 7.37 (1H, t, H8), 7.31 (1H, d, H4), 7.20 (1H, d, H7), 2.68 (3H, s, $COCH_3$). *Anal.* Calc. for $RuC_{22}H_{17}N_6OCl_2SBr$: C, 39.71; H, 2.58; N, 12.63. Found: C, 39.60; H, 2.31; N, 12.53%.

2.2. Instrumentation

C, H and N analyses were performed on an elemental analyzer EURO VECTOR model EA3000. IR spectra were acquired by FT-IR JASCO model 420. Electronic absorption spectra were recorded on a Shimadzu 240-UV–visible spectrophotometer at room temperature. The ^{1}H NMR spectra were measured on a Bruker-Avance 400 MHz spectrometer at 400 MHz using TMS as an internal standard. Electrochemical measurements were performed in acetonitrile (Aldrich, HPLC grade) using Volta Lab model PGP201 with a platinum disk working electrode (1.6-mm diameter), a platinum wire counter electrode and a silver wire pseudo-reference electrode. Ferrocene (0.665 V versus NHE) is used as an internal reference [23]. The temperature was controlled (at 25.0 ± 0.1 °C) by a Haake D8-G refrigerated. (TBAHF) was used as a supporting electrolyte, and the solution concentration was ca. 10^{-3} M.

2.3. Computational methods

All DFT calculations were carried out using GAUSSIAN03 program package [24]. The X-ray crystallographic structure for **3** complex was used as starting coordinates to generate *trans*-[Ru^{II}(L)(Azo)Cl_2] (**1**, **2**–**4**) geometries. The structures were then optimized using the Becke three parameters hybrid exchange [25] and the Lee–Yang–Parr correlation hybrid functional [26] (B3LYP). LanL2DZ effective core potential basis set was employed for Ruthenium and 6-31g* for the rest of the atoms in acetonitrile solution. Time-dependent density functional theory (TD-DFT) [27] and NBO analysis were performed using B3LYP functional and a mixed basis set, LanL2DZ/6-31+g(d,p), in acetonitrile as a solvent via polarized continuum model (PCM). The lowest 20 singlet-to-singlet spin-allowed excitation states were taken into account for the calculations of the electronic absorption spectrum for complex **3**. Orbital contribution was analyzed using GAUSSSUM software [28].

2.4. Crystallography

A suitable irregular brown flat fragment of approximate dimensions 0.47 × 0.15 × 0.13 mm^3 was mounted on a glass fiber and the data collected at room temperature employing enhanced Mo radiation, λ = 0.71073 Å, using Xcalibur/Oxford Diffractometer equipped with Eos CCD detector. CRYSALIS PRO software was used for data collection, absorption correction and data reduction [29]; 6 ω scan runs, 317 frames collected after optimization, average exposure time 64.04 s, 1° frame width, 45 mm detector distance. 'Multi-scan' absorption corrections were applied with Min and Max transmission factors of 0.214 and 1.000, respectively.

Cell parameters were retrieved using all observed reflections. The structure was solved using Olex2 [30] as $P21/c$ by direct methods and refined by least squares on F^2 to $R_1 = 0.0709$ [$I \geqslant 2\sigma(I)$] with $2\theta = 6.1–58.26°$. Subsequent re-solution and refinement was done using SHELXTL program package [31] and reduced $R_1 = 0.0524$ with θ full 25.03° and diffraction measurement fraction $\theta_{max} = 0.998$. Goodness-of-fit on $F^2 = 1.053$.

Molecular graphics and publication material were compiled using SHELXTL. All nonhydrogen atoms were refined anisotropically with the hydrogen atoms placed constrained and assigned isotropic thermal parameters of 1.2 times the riding atoms. Details of data collection and refinement are given in Table 1. An ORTEP drawing of the asymmetric unit (30% probability) is given in Fig. 1. There are two molecular units, $C_{23}H_{20}Cl_2N_6O_2RuS$, per asymmetric unit. The coordination sphere of Ru(II) is close to octahedral with the chloride anions trans to each other. The four equatorial sites are occupied by N atoms of the two ligands.

Table 1
Crystallographic data and structure refinement parameters for **3**.

Empirical formula	$C_{23}H_{20}Cl_2N_6O_2RuS$
Formula weight	616.484
Temperature (K)	293(2)
Wavelength (Å)	0.71073
Crystal system	monoclinic
Space group	$P\ 21/c$
Formula weight	616.484
Unit cell dimensions	
a (Å)	13.9609(10)
b (Å)	16.3913(11)
c (Å)	22.3177(14)
α (°)	90
β (°)	100.665(7)
γ (°)	90
Volume (Å^3)	5018.9(6)
Z	8
Density (calculated) (Mg/m^3)	1.632
Absorption coefficient (mm^{-1})	0.954
F(000)	2480
Crystal size (mm^3)	0.4725 × 0.1518 × 0.1301
Theta range for data collection (°)	3.05–25.03
Index ranges	$-16 \leqslant h \leqslant 16$, $-19 \leqslant k \leqslant 19$, $-26 \leqslant l \leqslant 26$
Reflections collected	25 964
Independent reflections	8870 [R(int) = 0.0409]
Completeness to theta = 25.03°	99.8%
Absorption correction	semi-empirical from equivalents
Max. and min. transmission	1.00000 and 0.21354
Refinement method	Full-matrix least-squares on F^2
Data/restraints/parameters	8870/0/621
Goodness-of-fit on F^2	1.053
Final R indices [$I > 2\sigma(I)$]	$R_1 = 0.0524$, $wR_2 = 0.1097$
R indices (all data)	$R_1 = 0.0901$, $wR_2 = 0.1330$
Largest diff. peak and hole (e Å^{-3})	0.766 and −0.666

$R_1 = \Sigma||F_o| - |F_c||/\Sigma|F_o|$; $wR_2 = \{\Sigma[w(F_o^2 - F_c^2)^2]/\Sigma[w(F_o^2)^2]\}^{1/2}$.

3. Results and discussion

3.1. Synthesis

The substituted azoimine ligands [3] and 2-(1,2,3-thiadiazol-4-yl)pyridine (**L**) [24] used in this study were prepared according to literature procedure. The ligand, 2-(1,2,3-thiadiazol-4-yl)pyridine (L), is not stable in the presence of light and was not used before to prepare mixed-ligand ruthenium complexes. The synthesis of *trans*-[Ru^{II}(L)(Azo)Cl$_2$] (**1–5**) was achieved by the stepwise equimolar addition of azoimine ligands, 2-(1,2,3-thiadiazol-4-yl)pyridine (**L**) and then an excess of lithium chloride (Scheme 1). The structures of the diamagnetic complexes were confirmed by ^{1}H NMR spectra and crystallography for monuclear *trans*-[Ru(C$_6$H$_5$N=NC(COCH$_3$)=NC$_6$H$_4$OCH$_3$)(L)Cl$_2$](**3**).

The IR spectra of complexes **1–5** exhibit a sharp bands at 1695–1705 cm^{-1} and intense bands at 1580–1610 and 1470–1490 cm^{-1} which correspond to acetyl group, C=N and N=N stretching bands, respectively.

3.2. Crystal structures

Complex **3** crystallizes in the monoclinic space group $P\ 21/c$. Crystallographic data are compiled in Table 1 and ORTEP drawing of **3** is shown in Fig. 1. In addition, selected inner coordination sphere bond parameters of **3** are listed in Table 2. Complex **3** is crystallized in two independent molecules with some minor differences in bond lengths and angles (Table 2). The ruthenium atom has the normal octahedral geometry, distorted only by the requirements imposed by the chelate rings. Interestingly, Ru–N(thiazole) (N(5) and N(11)) bond distances (average, 2.125 Å) is shorter than the Ru–N(pyridine) (N(4) and N(10)) bond distances (average, 2.162 Å), suggesting that thiazole ring is a strong σ-donor and π-acceptor ligand than pyridine. The azomethine ligand is known to interact strongly with the Ru(II) center via the dπ–π* interactions [21]. This has been reflected in the average Ru–N(L)

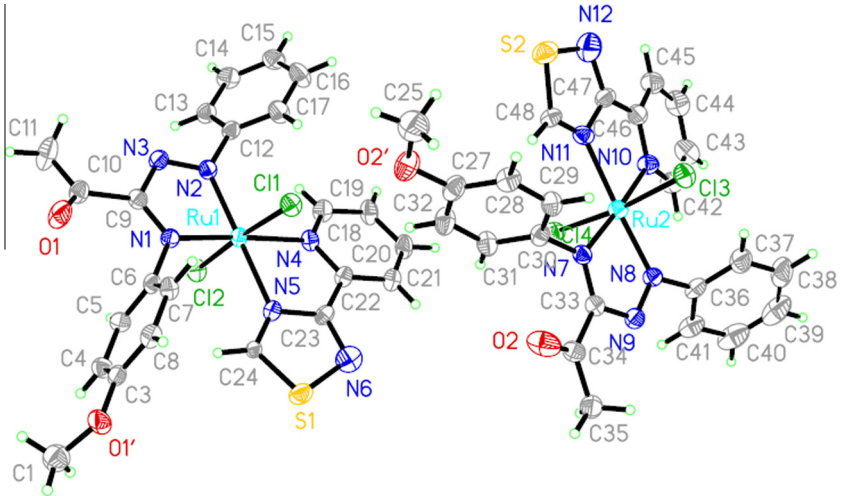

Fig. 1. Thermal ellipsoid drawing (30%) of complex **3** showing the two independent molecules of the Ru complex.

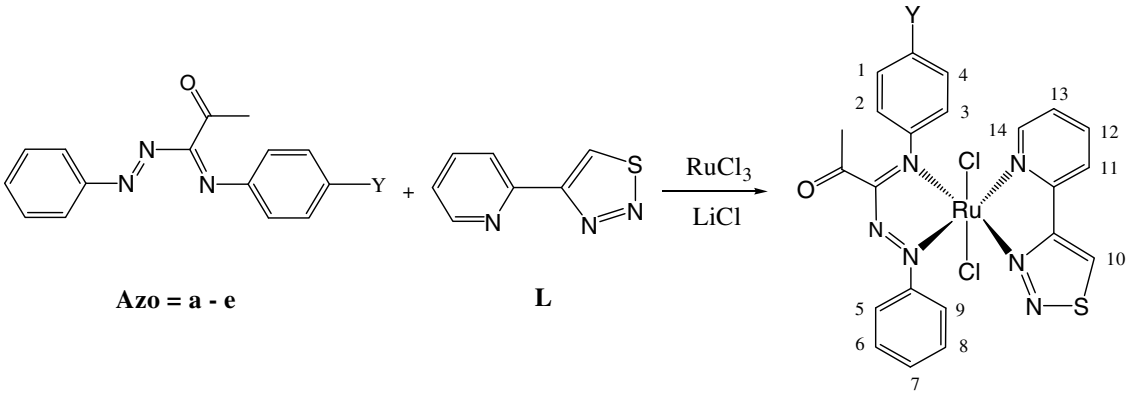

1 (Y=H); **2** (Y=CH_3); **3** (Y=OMe); **4** (Y=Cl); **5** (Y= Br)

Scheme 1.

Table 2
Bond lengths (Å) and angles (°) for complex **3.**

Molecule (**1**)		Molecule (**2**)	
Bond lengths (Å)		*Bond lengths (Å)*	
Ru(1)–N(2)	1.959(4)	Ru(2)–N(8)	1.962(5)
Ru(1)–N(1)	1.973(4)	Ru(2)–N(7)	1.974(4)
Ru(1)–N(5)	2.125(5)	Ru(2)–N(11)	2.124(5)
Ru(1)–N(4)	2.176(5)	Ru(2)–N(10)	2.148(5)
Ru(1)–Cl(1)	2.3643(15)	Ru(2)–Cl(3)	2.3634(16)
Ru(1)–Cl(2)	2.3822(15)	Ru(2)–Cl(4)	2.3851(16)
N(2)–N(3)	1.307(6)	N(8)–N(9)	1.306(6)
N(1)–C(9)	1.315(7)	N(7)–C(33)	1.321(7)
Bond angles (°)		*Bond angles (°)*	
N(2)–Ru(1)–N(1)	76.20(19)	N(8)–Ru(2)–N(7)	76.83(19)
N(2)–Ru(1)–N(5)	177.21(19)	N(8)–Ru(2)–N(11)	176.11(19)
N(1)–Ru(1)–N(5)	102.01(18)	N(7)–Ru(2)–N(11)	102.55(19)
N(2)–Ru(1)–N(4)	106.05(18)	N(8)–Ru(2)–N(10)	104.36(19)
N(1)–Ru(1)–N(4)	176.48(18)	N(7)–Ru(2)–N(10)	174.23(19)
N(5)–Ru(1)–N(4)	75.84(18)	N(11)–Ru(2)–N(10)	76.65(19)
Cl(1)–Ru(1)–Cl(2)	175.08(6)	Cl(3)–Ru(2)–Cl(4)	173.39(6)

(2.118 Å) and Ru–N(Azo) (average, 1.961 Å) and the Ru–N(methine) (average, 1.974 Å). The shortening in the bond length for Ru–Azo by 0.151 Å compared to Ru–L indicates that the M–L π interaction is localized in the M–Azo fragment [32]. However, it is interesting to note that the bond lengths Ru–N(Azo) and Ru–N(methine) for complex **3** are slightly shorter while the N=N 1.307(6) Å is longer than the corresponding lengths for similar reported ruthenium azoimine complexes *trans*-[Ru(Azo)(t-bpy)Cl_2] (Ru–N(azo) = 1.958 (4) Å, Ru–N(methine) = 1.988(4) Å and N=N is 1.252(11) Å [33]) and *trans*-[Ru(Az)(bpy)Cl_2] (Ru–N(azo) = 1.965(3) Å, Ru–N(imine) = 2.002(3) Å [34]). The greater π-back donation for **3** suggests that the ligand 2-(1,2,3-thiadiazol-4-yl)pyridine (L) is a better σ-donor compared to bpy derivatives. In the equatorial plane, the five membered rings described by the coordination of an azoimine ligand (average, 76.5(19°)) and of 4,4′-bi-1,2,3-thiadiazole (average, 76.1 (19°)) to ruthenium have approximately equivalent coordination bite-angles (Table 2) and deviate from ideal octahedral geometry. The average bond angles for Cl–Ru–Cl (174.2(6)°) which is less than the ideal 180° might be due to repulsion of the Ru–Cl bond by one of the twisted phenyl rings of the Azo ligand.

3.3. Electrochemistry

Electrochemical properties of **1–5** have been studied by cyclic voltammetry in acetonitrile using 0.1 M TBAHF as supporting electrolyte. The results are summarized in Table 3 and a representative voltammogram for **3** is depicted in Fig. 2. Complexes **1–5** exhibited a quasireversible oxidative response in the range 1.31–1.38 V, which has been assigned to Ru(III/II) oxidations. The two one-electron ligand reduction waves between −0.39 and −0.80 V vs. NHE (cathodic wave peak maxima) are assigned to the two electron reduction of the azo group. The large anodic shift (150 mV) for this family (compared to the *trans*-[Ru(Azo)(bpy)Cl_2] complexes [3]) resulted from replacing one of the pyridine ring by

Table 3
Cyclic voltammetry and electronic spectroscopy data of *trans*-[Ru^{II}(L)(Azo)Cl_2] (**1–5**).[a]

Complex	Ru(III/II)	Azo(0/−)[b]	Azo(−/2−)[b]	Electronic spectra λ_{max} (nm) [c]
1	1.27	−0.44	−0.71	505
2	1.25	−0.45	−0.76	503
3	1.23	−0.47	−0.80	507
4	1.35	−0.39	−0.65	509
5	1.31	−0.40	−0.67	511

[a] Solvent MeCN, supporting electrolyte Bu_4NPF_6 (0.1 M), scan rate 0.1 V s, Pt-disk working electrode, Pt-wire auxiliary electrode, reference electrode Ag at 25 °C.
[b] The cathodic peak maximum.
[c] Solvent MeCN.

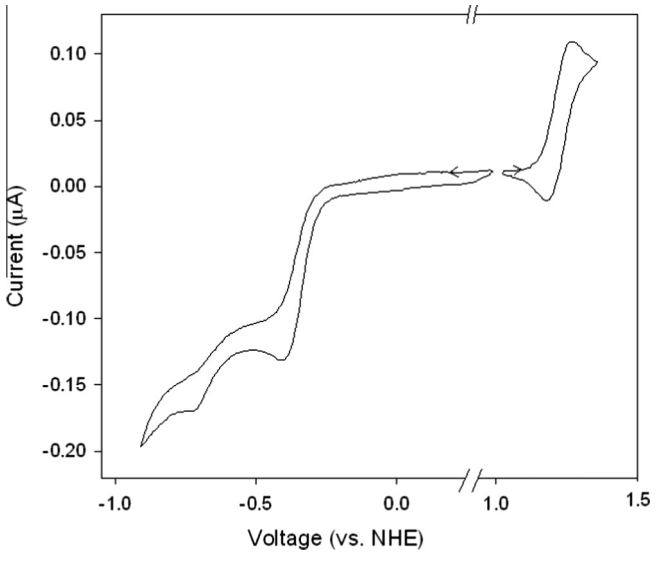

Fig. 2. Cyclic voltammogram for complex **3** in acetonitrile, 0.1 M TBAH at 25 °C, data reported in V vs. NHE with scan rate of 0.1 V/s.

strong π-excessive thiadiazoles ring. For the five complexes, the potential of the Ru(III/II) couple is slightly affected by changing the substituent Y on the azoimine ligand (Azo). The Ru(III/II) couple for complex **1** was used to find the ligand electrochemical parameters (E_L(L) = 0.46) 4,4′-bi-1,2,3-thiadiazole ligand by using the previously found (E_L(Azo) = 0.42) [3], E_L(Cl) = −0.24 [35]) and Lever method [35]. The parameter E_L reflects the stabilizing effect of the ligands on the Ru(II) state and so the greater value of E_L, the more positive the Ru(III/II) couple.

4. Electronic structure

Electronic absorption spectra of the complexes **1–5** were acquired in acetonitrile at room temperature and the resulting data are summarized in Table 3. Complex **3** displayed intense bands in the UV–Vis region (Fig. 3). An analogous general trend has been observed in the electronic absorption spectra of all the complexes. These bands are assigned based on the closest agreement between the experimental spectrum and the theoretical spectrum obtained by TD-DFT calculations (Fig. 3).

Theoretical calculations were performed on **3**; relative percentages of atomic contributions to the lowest unoccupied and highest occupied molecular orbitals have been placed in Table S4. Moreover, the isodensity plots for the HOMOs and LUMOs orbitals are shown in Fig. 4. The lower unoccupied molecular orbitals (LUMOs) consist mostly of a series of antibonding π* orbital of azoimine and L. Results indicate that the HOMO constructed mainly from t_2g Ru orbitals (62%) while LUMO is constructed from the π* orbital of azoimine (68%) with 24% metal d-orbital in character which suggests significant back donation [36].

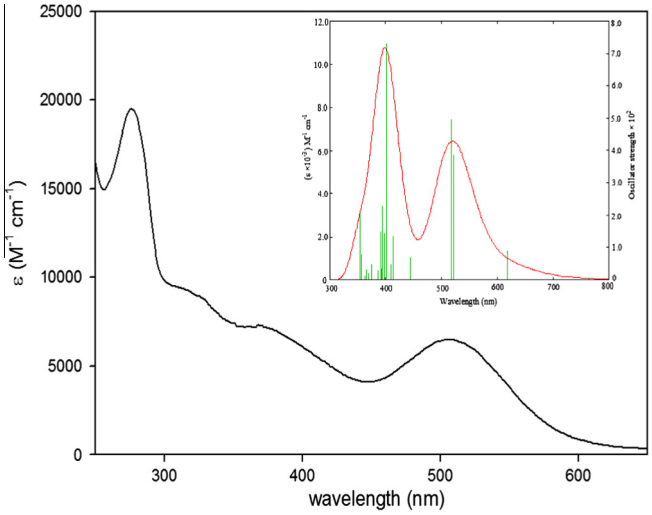

Fig. 3. UV–Vis spectrum for **3** in acetonitrile. Inset shows simulated absorption spectrum. (Black line) based on TD-DFT calculations, compared to excitation energies and oscillator strengths.

The lowest 20 singlet-to-singlet spin-allowed excitation states were taken into account for the calculation of the electronic absorption spectrum of complex **3** using TD-DFT method. Excitation energies, oscillator strengths and corresponding transitions compositions for the simulated absorption bands in acetonitrile solution are listed in Table S5. Fig. 3 shows that the simulated and experimental spectra of complex **3** in acetonitrile.TD-DFT calculations show that the band centered at λ_{max} = 507 nm (experimentally) which is resulted from the overlap of two MLCT transition (≈518 and 522 nm (calculated)). These transitions are resulted from the (HOMO, HOMO−2) orbitals, which have a sizable contributions of Ru(dπ) orbitals, to LUMO and LUMO+3 which has a significant contribution from the π* orbital of azomethine; thus these two transitions are assigned to MLCT (Ru(dπ) → π* azomethine). In the near-UV region, the band centered at 383 nm (experimentally) (≈395 nm (calculated)) arises from the overlap of two transition; π → π* arises from (HOMO−8, HOMO−6 and HOMO−2 to LUMO).

For this family *trans*-[Ru^{II}(L)(Azo)Cl_2] (**1–5**), there is a small shift in the Ru(III/II) couple and the energy of the MLCT band upon replacing the electron donating group Y (CH_3) in the azoimine ring by electron withdrawing groups (Cl, Br). The small shift can be explained by the small changes in the energy of the orbitals involved in MLCT (HOMO's and the LUMO azoimine ligand) and Ru(III/II) couple (HOMO's) events (see Table S4).

5. Conclusions

Five novel mononuclear *trans*-[Ru(L)(Azo)(Cl_2)] ({Azo = C_6H_5 N═NC($COCH_3$)═NC_6H_4Y, Y = H (**1**), CH_3 (**2**), OCH_3 (**3**), Cl (**4**), Br (**5**) and L is 2-(1,2,3-thiadiazol-4-yl)pyridine have been synthesized. Assuming ligand additively, the Ru(III/II) couple for these octahedral complexes was used to find the ligand electrochemical parameter (E_L(L)) for unreported 2-(1,2,3-thiadiazol-4-yl)pyridine ligands (L) to be 0.46. The electronic absorption spectra of these complexes show strong MLCT band in the visible. This band is assigned to a (Ru(II)-to-azomethine) MLCT transitions based on TD-DFT calculations.

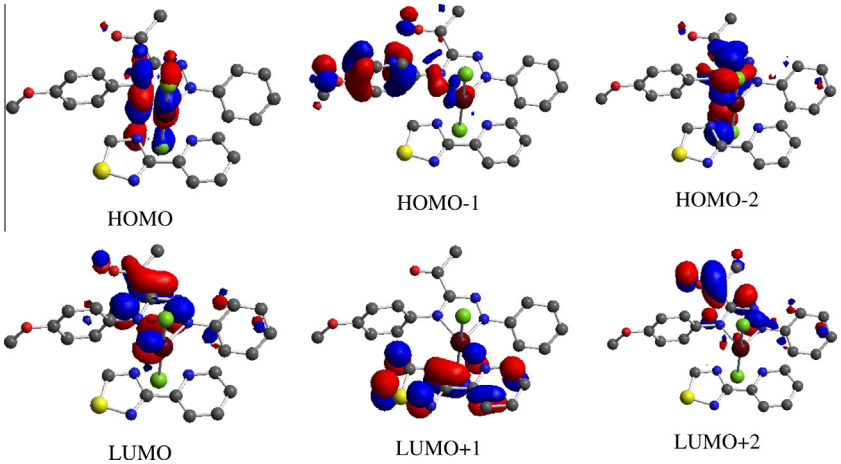

Fig. 4. Isodensity plots of the HOMO and LUMO orbitals of complex **3**.

Acknowledgements

This paper was funded by the Deanship of Research (DSR), King Adulaziz University, Jeddah, under grant No. (430/662/1432). The authors, therefore, acknowledge with thanks DSR technical and financial support. Also The financial support of Hashemite university is gratefully acknowledged.

Appendix A. Supplementary data

Supplementary data associated with this article can be found, in the online version, at http://dx.doi.org/10.1016/j.ica.2013.02.003.

References

[1] F. Blau, Chem. Ber. 21 (1888) 1077.
[2] E.C. Constable, Adv. Inorg. Chem. 34 (1989) 1.
[3] M. Al-Noaimi, H. Saadeh, S. Haddad, M. El-Barghouthi, M. El-khateeb, R.J. Crutchley, Polyhedron 26 (2007) 3675.
[4] M. Al-Noaimi, M. El-khateeb, S. Haddad, M. Sunjuk, R. Crutchley, Polyhedron 27 (2008) 3239.
[5] M. Al-Noaimi, R. Abdel-Jalil, S. Haddad, R. Al-Far, M. Sunjuk, R.J. Crutchley, Inorg. Chim. Acta 359 (2006) 2395.
[6] M. Al-Noaimi, M. El-Barghouthi, M. El-khateeb, O. Abdel-Rahman, H. Görls, R.J. Crutchley, Polyhedron 27 (2008) 2698.
[7] M. Al-Noaimi, M. El-khateeb, S. Haddad, H. Saadeh, Transition Met. Chem. 35 (2010) 877.
[8] M. Al-Noaimi, M.I. El-Barghouthi, O.S. Abdel-Rahman, S.F. Haddad, A. Rawashdeh, Polyhedron 30 (2011) 1884.
[9] E.C. Constable, P.J. Steel, Coord. Chem. Rev. 93 (1989) 205.
[10] S. Srivastava, V. Srivastava, K. Chaturvedi, O.P. Pandey, S.K. Sengupta, Thermochim. Acta 240 (1994) 101.
[11] A. Louria, J. Heterocycl. Chem. 37 (2000) 747.
[12] Z.A. Hozien, A.O.S. Abd El-Wareth, H.A.H. El-Sherief, A.M. Mahmoud, J. Heterocycl. Chem. 37 (2000) 943.
[13] Z.H. Chohan, M.F. Jaffery, C.T. Supuran, Met. Drugs 8 (2001) 95.
[14] A. Mastrolorenzo, C.T. Supuran, Met. Drugs 7 (2000) 49.
[15] K. Miyamoto, R. Koshiura, M. Mori, H. Yokoi, C. Mori, T. Hasegawa, K. Takatori, Chem. Pharm. Bull. 33 (1985) 5126.
[16] H.N. Jayaram, W. Zhen, K. Gharehbaghi, Cancer Res. 53 (1993) 2344.
[17] E.S. Raper, Coord. Chem. Rev. 129 (1994) 91.
[18] G. Alzuet, J. Casanova, J.A. Ramirez, J. Borrs, O. Carugo, J. Inorg. Biochem. 57 (1995) 219.
[19] G. Alzuet, L. Casella, A. Perotti, J. Borrs, J. Chem. Soc., Dalton Trans. (1994) 2347.
[20] Z.H. Chohan, S. Kausar, Drugs 7 (2000) 17.
[21] M. Zolfigol, M. Bagherzadeh, S. Mallakpour, G. Chehardoli, A. Ghorbani-Choghamarani, N. Koukabi, M. Dehghanian, Doroudgar J. Mol. Catal. A: Chem. 270 (2007) 219.
[22] E. Cerrada, M. Laguna, N. Lardíes, Eur. J. Inorg. Chem. (2009) 137.
[23] T. Gennett, D.F. Milner, M.J. Weaver, J. Phys. Chem. 89 (1985) 2787.
[24] M.J. Frisch et al., GAUSSIAN 03, Revision D.01, Gaussian, Inc., Wallingford CT, 2004.
[25] A.D. Becke, J. Chem. Phys. 98 (1993) 5648.
[26] C. Lee, W. Yang, R.G. Parr, Phys. Rev. B 37 (1988) 785.
[27] M.K. Casida, in: Recent Advances in Density Functional Methods, Part I, in: D.P. Chong (Ed.), Recent Advances in Computational Chemistry, vol. 1, World Scientific, Singapore, 1995, p. 155.
[28] N.M. O'Boyle, A.L. Tenderholt, K.M. Langner, J. Comput. Chem. (2008) 29.
[29] CRYSALISPRO, Agilent Technologies, Version 1.171.35.11 (release 16–05-2011 CrysAlis171.NET) (compiled May 16, 2011).
[30] O.V. Dolomanov, L.J. Bourhis, R.J. Gildea, J.A.K. Howard, H. Puschmann, J. Appl. Crystallogr. 42 (2009) 339.
[31] G.M. Sheldrick, SHELXTL Version 6.10 Structure Determination Software Suite, Bruker AXS Inc., Madison, WI, 2000.
[32] L. Goswami, F. Falvello, A. Chakravorty, Inorg. Chem. 26 (1987) 3365.
[33] M. Al-Noaimi, B.F. Ali, A. Rawashdeh, Z. Judeh, Polyhedron 29 (2010) 3214.
[34] M. Al-Noaimi, M. El-khateeb, H. Görls, Acta Crystallogr., Sect. E 63 (11) (2007) m2713.
[35] A.B. Lever, Inorg. Chem. 29 (1990) 1271.
[36] S.I. Gorelsky, A.B.P. Lever, M. Ebadi, Coord. Chem. Rev. 230 (2002) 97.